Proc. of the European Safety and Reliability Conference (ESREL 2026)
Edited by José C. Matos, Paulo B. Lourenço, Michael Beer, Daniel Oliveira, Edoardo Patelli, Hélder S. Sousa, Rui A. Silva and Monica Santamaria

doi: 10.3850/ESREL2026061419_esrel26-p26177-cd

A Fuzzy Logic–Based Model Predictive Control Framework for Risk-Aware Safety Control of Railway Virtual Coupling

Yiran Gu
School of Automation and Intelligence, Beijing Jiaotong University, China. E-mail: 24120197@bjtu.edu.cn

Yiling Wu
School of Automation and Intelligence, Beijing Jiaotong University, China. E-mail: 21120255@bjtu.edu.cn

Fei Yan
School of Automation and Intelligence, Beijing Jiaotong University, China. E-mail: fyan@bjtu.edu.cn

Virtual Coupled Train Sets (VCTS) achieve cooperative operation through inter-train communication; however, under real-world operating conditions, multi-source operational risks pose significant challenges to coordination and safety. To address this issue, this paper proposes a multi-layer risk-aware reference generation and control framework for VCTS to enhance the operational safety of train formations. Within this framework, VCTS is abstracted as a leader–follower train structure, and the multi-source risks faced by the following train are categorized into leader-train system-level risk, environmental risk, and communication risk. Specifically, the leading train employs a Bilateral Cumulative Sum (Bi-CUSUM)-based module to predict its system-level risk and transmit it to the following train. The following train then integrates the leader's system-level risk, onboard-perceived environmental risk, and communication risk using a fuzzy logic approach based on the analytic hierarchy process (AHP), resulting in a comprehensive risk assessment index. Based on this index, a dynamically generated, risk-adaptive target speed serves as the reference for a receding-horizon Model Predictive Control (MPC) scheme, enabling safe and conservative longitudinal behavior under dynamic operating conditions. Simulation results demonstrate that the proposed framework is capable of providing safe and robust control performance under elevated risk conditions.

Keywords: Virtually Coupled Train Sets, Risk-Aware Control, Fuzzy Logic, AHP, Bi-CUSUM, MPC

1. Introduction

The rapid growth of urbanization leads to increasing demands on rail transit systems for higher transport capacity, improved energy efficiency, and enhanced operational flexibility. To address these requirements, Virtual Coupled Train Sets (VCTS) have emerged as a promising train operation paradigm Xun et al. (2022). Unlike conventional mechanical coupling, VCTS enable multiple trains to operate cooperatively in a platoon with reduced inter-train headways through dedicated inter-train communication and cooperative control strategies. This virtual coupling mechanism supports dynamic coupling and decoupling during operation, thereby improving line capacity and service frequency.

A fundamental prerequisite for safe and efficient VCTS operation is the reliability of inter-train information exchange. Accurate state perception and synchronized control are essential to maintain ultra-close following distances while ensuring operational safety. However, in practical operating environments, the following train is subject to multi-source operational risks, which may significantly affect state awareness and decision-making, thereby posing challenges to the safe and coordinated operation of train formations.

Existing cooperative control methods for virtually coupled trains have made significant progress in improving longitudinal coordination and safety by leveraging inter-train communication and distributed control architectures. Representative studies include distributed nonlinear cooperative control under moving block systems Ning et al. (2018), robust and constrained model predictive control frameworks Felez et al. (2022); Su et al. (2022), as well as cooperative collision-avoidance control strategies Su et al. (2022). These approaches demonstrate improved performance in handling disturbances, model uncertainties, and actuator limitations through robust or constraint-aware control designs Zhu et al. (2024).

Despite these advances, most existing methods implicitly assume the availability of timely and accurate leader-state information transmitted over reliable communication links, ensuring continuous observability of the leader's motion. In realistic virtual coupling scenarios, stochastic communication degradation and observation uncertainty can significantly impair state awareness. More importantly, the resulting risk conditions are rarely modeled explicitly or integrated into control decision-making, leaving cooperative control strategies largely decoupled from real-time risk assessment and potentially compromising safety and performance.

To address this challenge, this paper proposes a risk-aware safety control framework that integrates multi-source risk perception with a receding-horizon Model Predictive Control (MPC) scheme. Multi-source risks associated with the leading train's system-level condition, environmental disturbances, and communication quality are fused into a unified risk assessment index using a fuzzy logic scheme. This index is used to generate a conservative, risk-adaptive target speed, which serves as the reference for the MPC controller to regulate the longitudinal motion of the following train. In this way, safety considerations are explicitly incorporated while maintaining smooth and accurate speed tracking performance. Simulation results under elevated risk levels demonstrate that the proposed framework provides safe and robust longitudinal control for virtually coupled train operations.

2. Model Construction

2.1. *Train Dynamics Model*

The longitudinal motion of the following train is modeled as a single-point mass system in the discrete-time domain. According to Newton's second law, the longitudinal acceleration of the train at time step i is given by

$$a_i = \frac{1}{m}\left(u_i - r(v_i) - mg\sin\left(\theta(x_i)\right)\right) \tag{1}$$

where m denotes the equivalent mass of the train, u_i represents the traction force, v_i is the train speed, and $\theta(x_i)$ denotes the track gradient at position x_i.

The basic running resistance $r(v_i)$ is described by the Davis equation:

$$r(v_i) = a + bv_i + cv_i^2 \tag{2}$$

where a, b, and c are the coefficients corresponding to rolling resistance, viscous resistance, and aerodynamic drag, respectively.

The longitudinal kinematic variables of the train, including position, speed, and acceleration, are consolidated into a state vector

$$k_i = (x_i,\ v_i,\ a_i)^\top \tag{3}$$

Using a forward Euler discretization scheme, the train dynamics can be expressed as

$$\begin{bmatrix} x_{i+1} \\ v_{i+1} \end{bmatrix} = \begin{bmatrix} x_i \\ v_i \end{bmatrix} + dt \begin{bmatrix} v_i \\ a_i \end{bmatrix} \tag{4}$$

where dt denotes the sampling interval.

Accordingly, Eqs. (1)–(4) can be compactly written in the following state-space form:

$$k_{i+1} = f(k_i, u_i) \tag{5}$$

2.2. *System Configuration of the Virtual Coupling Train System*

To focus on the core control strategy, the VCTS architecture is abstracted into a simplified leader–follower configuration, as illustrated in Fig. 1. The system consists of two primary units: the leading train (Leader) and the following train (Follower).

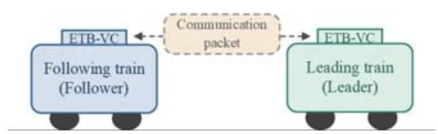

Fig. 1. Simplified architecture of the virtual coupling train system

In this configuration, the leading train acts as the information source, while the following train operates as the ego train. Inter-train coordination is achieved via a train-to-train communication link implemented over the Ethernet Train Backbone

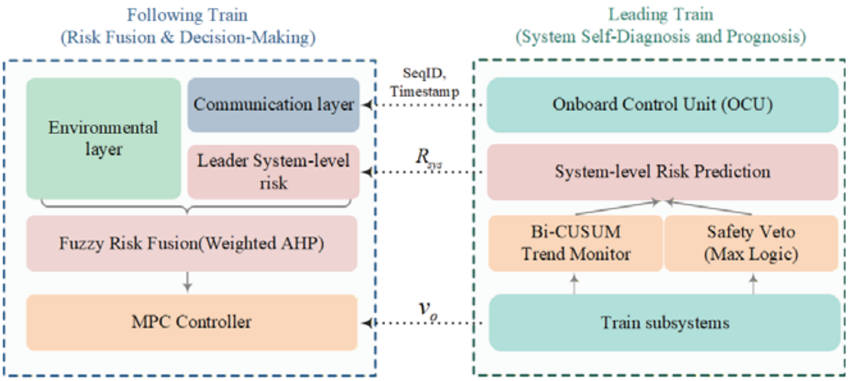

Fig. 2. Framework of the proposed method.

for Virtual Coupling (ETB-VC). The leading train transmits key operational information to the following train, based on which the follower adjusts its longitudinal motion to ensure safe and efficient virtual coupling operation.

2.3. *Multi-source Risk Classification for Trains*

The multi-source operational risks of trains are classified into three layers: the system layer, the environmental layer, and the communication layer. This classification is consistent with established literature and prevailing railway safety and operation frameworks, which analyze train operation from the perspectives of onboard system functionality, external operating conditions, and information transmission reliability Palo (2014); Germoglio Barbosa et al. (2024); Farooq and Soler (2017); de Loizaga and Martin (2024); Kong et al. (2023).

As summarized in Table 1, these three layers capture onboard subsystem vulnerabilities, infrastructure-related environmental conditions, and train-to-train communication reliability, respectively. This layered classification provides a systematic foundation for subsequent risk modeling and decision-making in VCTS.

Building upon the proposed multi-layer risk classification, a heterogeneous risk-aware fusion and control framework is developed, as illustrated in Fig. 2, to support safe virtual coupling operations. The overall operational risk is decomposed

Table 1. Multi-source information classification for trains

Layer	**Risk Factor**
System	Automatic Train Protection (ATP)
	Automatic Train Operation (ATO)
	Sensors
	Braking system
	Traction system
	Train Control and Monitoring System (TCMS)
Environment	Track gradient
	Wheel–rail adhesion
	Visibility
Communication	Transmission latency
	Jitter
	Packet loss

into system-level, environmental, and communication components. Owing to asymmetric perception capabilities, the system-level risk is assessed by the leading train through onboard self-diagnosis, while environmental and communication risks are evaluated by the following train using local perception and received train-to-train information.

Specifically, the leading train employs a Bilateral Cumulative Sum (Bi-CUSUM)-based trend monitor to detect system-level risk variations and generate a conservative short-horizon risk prediction, denoted as R_{sys}. This prediction is transmitted to the following train together with structured communication metadata and the observed speed v_o of the leading train, thereby providing both risk-related and kinematic information for downstream decision-making and control.

The following train then fuses system, environmental, and communication risks via an Analytic Hierarchy Process (AHP)-based fuzzy logic scheme, yielding an integrated risk index. This index is embedded within an MPC-based control framework to enable the synthesis of conservative, risk-aware longitudinal control policies.

2.4. *Hierarchical Risk Fusion and Transmission Dilemma*

The raw indicators associated with the risk factors listed in Table 1 are initially collected in their native physical units and subsequently normalized to ensure comparability across heterogeneous data sources. Each normalized indicator ξ is then mapped to a fuzzy membership degree $\mu(\xi) \in [0, 1]$ using trapezoidal membership functions, which are widely adopted in multi-criteria risk assessment frameworks.

For each risk layer l, a layer-wise risk score R_l is obtained via centroid defuzzification, as defined in Eq. (6),

$$R_l = \frac{\int_{\mathcal{D}_l} \xi \, \mu_{\text{agg}}(\xi) \, d\xi}{\int_{\mathcal{D}_l} \mu_{\text{agg}}(\xi) \, d\xi} \tag{6}$$

where $\mathcal{D}_l$ denotes the universe of discourse associated with layer l, and μ_{agg} represents the aggregated membership function obtained through a Mamdani-type fuzzy inference mechanism using max–min aggregation. The layer index $l \in \{\text{sys}, \text{env}, \text{comm}\}$ corresponds to the system, environmental, and communication layers, respectively.

Fusion weights $\mathbf{W} = \big[w_{\text{sys}},\, w_{\text{env}},\, w_{\text{comm}}\big]^\top$ are obtained from an expert-elicited pairwise comparison matrix, in which domain experts assess the relative importance of different risk layers. The resulting matrix is validated through a consistency ratio (CR) check, and the derived weights are considered acceptable when $\text{CR} < 0.1$.

Based on the above hierarchical fusion mechanism, the following train integrates the system-layer risk transmitted from the leading train with locally evaluated environmental and communication risks to compute the final comprehensive risk index R_{final}. The final risk is obtained as a weighted summation of the individual layer-wise risks, as expressed in Eq. (7),

$$R_{\text{final}} = \sum_{l \in \{\text{sys,env,comm}\}} w_l \, R_l \tag{7}$$

where w_l denotes the relative importance weight associated with the l-th risk layer.

2.5. *Risk Trend Detection and Asymmetric Fail-Safe Prediction*

In tunnel environments or under severe wireless interference, intermittent communication degradation may prevent the following train from continuously acquiring the real-time system-layer risk R_{sys} of the leading train. To address this challenge, a conservative onboard risk trend detection and fail-safe prediction mechanism is deployed on the leading train, enabling robust forecasting of system-layer risk under communication uncertainty.

Rather than relying solely on absolute health values, the proposed approach monitors the temporal evolution of system health. Specifically, a sliding window of length N is employed to estimate the health gradient, as defined in Eq. (8),

$$g(i) = \frac{H(i) - H(i-N)}{N dt} \tag{8}$$

where $H(i)$ denotes the aggregated system health indicator at time step i. The gradient $g(i)$ characterizes short-term deterioration or recovery trends in system health.

Based on the estimated gradient $g(i)$, a Bi-CUSUM scheme is employed to detect statistically significant trend changes. The Bi-CUSUM statistics are updated according to Eq. (9),

$$\begin{aligned} S_{\text{lo}}(i) &= \max\big(0,\ S_{\text{lo}}(i-1) - g(i) - \delta\big) \\ S_{\text{hi}}(i) &= \max\big(0,\ S_{\text{hi}}(i-1) + g(i) - \delta\big) \end{aligned} \tag{9}$$

where δ is a slack parameter introduced to suppress minor fluctuations and sensor noise. A deterioration trend (or a recovery trend) is identified when $S_{\text{lo}}(i) > h$ (or $S_{\text{hi}}(i) > h$), respectively, with h denoting the decision threshold.

To prevent critical failures from being masked during aggregation, a veto mechanism is incorporated, such that abnormal escalation of any safety-critical subsystem directly dominates the aggregated system-layer risk assessment.

Once a trend change is detected according to Eq. (9), an asymmetric fail-safe prediction strategy is activated over a prediction horizon T_p. The predicted system health trajectory is defined in a phase-dependent manner, as expressed in Eq. (10),

$$H_{\text{pred}}(i+\tau) = \begin{cases} H(i) + \alpha\, g(i)\, \tau & \text{I} \\ H(i) - \beta\, \Phi(g(i), \tau) - \gamma & \text{II} \\ H(i) & \text{III} \end{cases} \tag{10}$$

where $\tau \in [0, T_p]$ denotes the prediction offset. The parameter $\alpha > 1$ amplifies early-warning signals during Phase I, whereas β and γ denote a damping factor and a safety margin during Phase II, respectively. Phase III corresponds to nominal operating conditions. The damping function $\Phi(\cdot)$ is defined in Eq. (11),

$$\Phi(g(i), \tau) = \max(0, g(i))\ \tau \tag{11}$$

which enforces conservative recovery prediction by preventing overly optimistic health restoration.

To further enhance robustness, a recovery-hold mechanism is introduced to maintain pessimistic predictions for a predefined duration after a recovery trend is detected. Finally, to guarantee fail-safe behavior under communication degradation, the predicted system health is constrained by a conservative pessimistic envelope, as given in Eq. (12),

$$H_{\text{pred}} \le H_{\text{real}} - \epsilon \tag{12}$$

where H_{real} denotes the true health level of the leading train subsystem and ϵ represents a predefined safety margin. This constraint enforces conservative underestimation of system health, thereby preventing premature relaxation of safety control actions. The resulting predicted health trajectory H_{pred} is subsequently mapped to the system-layer risk index R_{sys} via the fuzzy inference framework described in the previous section.

3. Risk-Aware Control via MPC

Risk-Aware Cost Function Rather than tracking a fixed or purely kinematic reference, the MPC controller for the following train follows a dynamically generated target speed v_{target} that explicitly embeds predictive risk awareness.

Under nominal operating conditions, when the synthesized risk R_{final} remains sufficiently low and no persistent degradation trend is detected, the target speed is set equal to the observed speed of the leading train. This strategy enables efficient and cooperative car-following behavior of the following train while maintaining smooth longitudinal control.

As R_{final} increases and a deterioration trend is identified by the Bi-CUSUM mechanism, the reference generation strategy transitions to a risk-dominant operating regime. In this regime, the target speed of the following train is no longer governed by the leading train but is instead regulated according to a risk-adaptive update law, ensuring a proactive and fail-safe reduction of the commanded speed.

To quantitatively incorporate the synthesized risk level into the reference generation process, a normalized risk factor $\eta \in [0, 1]$ is defined as

$$\eta = \text{clip}\left(\frac{R_{\text{final}} - R_{\text{low}}}{R_{\text{high}} - R_{\text{low}}}, 0, 1\right) \tag{13}$$

where R_{low} and R_{high} denote the lower and upper bounds of acceptable risk levels, respectively.

Based on the normalized risk factor, the target speed is updated incrementally as

$$v_{\text{target}} \leftarrow v_{\text{lim}} + \left[\kappa(1-\eta) - \lambda\right] dt \tag{14}$$

where v_{lim} denotes the stored line speed limit, κ controls the nominal acceleration tendency under low-risk conditions, λ introduces a conservative deceleration bias under elevated risk, and dt represents the discrete-time sampling interval.

The resulting control problem is solved online using a receding-horizon MPC scheme to obtain a risk-aware longitudinal control policy.

Over a prediction horizon of length N_p, the

MPC objective is formulated as

$$\min_{\{u_i\}_{i=0}^{N_p-1}} \sum_{i=0}^{N_p-1} J_i \tag{15}$$

The stage cost J_i is defined as

$$J_i = W_v \left(v_i - v_i^{\text{target}}\right)^2 + W_j \left(a_i - a_{i-1}\right)^2 \tag{16}$$

where W_v and W_j weight the speed tracking penalty and the acceleration smoothness penalty, respectively.

The MPC optimization is subject to the system dynamics and safety constraints:

$$k_{i+1|i} = f(k_{i|i}, u_{i|i}), \quad x_{i+1|i}^{\text{follower}} \le x_{i+1|i}^{\text{leader}} - d_{\text{safe}} \tag{17}$$

where x^{leader} denotes the longitudinal position of the leading train, x^{follower} denotes the longitudinal position of the following train, and d_{safe} denotes the minimum safety margin. All simulations are conducted on a platform equipped with an Intel Core i7-13700H processor and 16 GB RAM.

4. Experiment

4.1. *Scenario Description*

This study simulates a simplified VCTS comprising one leading train and one following train entering a tunnel, after which environmental and communication-layer risks increase.

In addition, the leading train experiences a transient traction overheat protection event, resulting in a temporary speed reduction followed by recovery, thereby representing a system-layer degradation scenario.

The simulation parameters are summarized in Table 2; parameters not listed are assumed to operate under nominal conditions.

Table 2. Environmental Changes in Simulation.

Parameter	Open Track → Tunnel	Unit
Aerodynamic Drag	$5.0 \rightarrow 8.0$	N/(m/s)^2
Adhesion	$1.0 \rightarrow 0.7$	–
Packet Loss	$0 \rightarrow 5\%–40\%$	–

4.2. *System-Level Risk Modeling and Prediction for the Leading Train*

To evaluate the proposed framework, the evolution of the health index of the leading train's traction system during an overheating protection process is simulated, as illustrated in Fig. 3(a). The simulated degradation and recovery process includes traction derating, protection trip, and system recovery, whose temporal progression is explicitly reflected in the health profile.

As shown in Fig. 3(b), the blue curve represents the real-time system-level risk of the leading train, while the red dashed curve denotes the predicted risk generated by the proposed method. The predicted risk exhibits a faster response to degradation events and consistently envelopes the real-time risk throughout the entire process, thereby providing a conservative safety margin for fail-safe decision-making.

By jointly examining Fig. 3(b) and (c), it is observed that this behavior is enabled by the proposed Bi-CUSUM-based trend detection mechanism. The negative and positive CUSUM responses allow timely identification of both degradation and recovery dynamics, ensuring rapid risk response while maintaining sufficient conservativeness.

4.3. *Resilient Risk Fusion and Safety Control of the Following Train*

This subsection evaluates the performance of the following train's risk fusion module and its safety response under combined tunnel-induced disturbances and leader system degradation.

Robustness of Multi-source Risk Fusion. As shown in Fig. 4, upon tunnel entry at $t = 200$ s, environmental degradation and severe communication jitter are immediately reflected in the layer-wise risk inputs. Despite channel noise, the predicted system-level risk transmitted from the leading train is successfully captured at approximately $t = 400$ s. As illustrated in Fig. 4(b), the final fused risk effectively suppresses high-frequency communication fluctuations during nominal operation, while responding promptly to system-level risk surges. This behavior demonstrates that the proposed fusion logic achieves fault dominance,

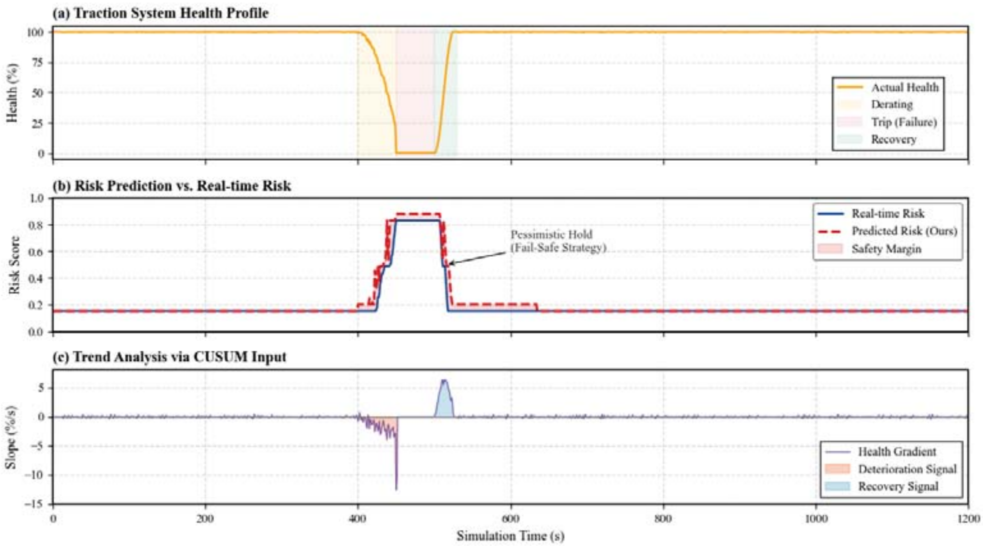

Fig. 3. **Validation of Risk Prediction.**

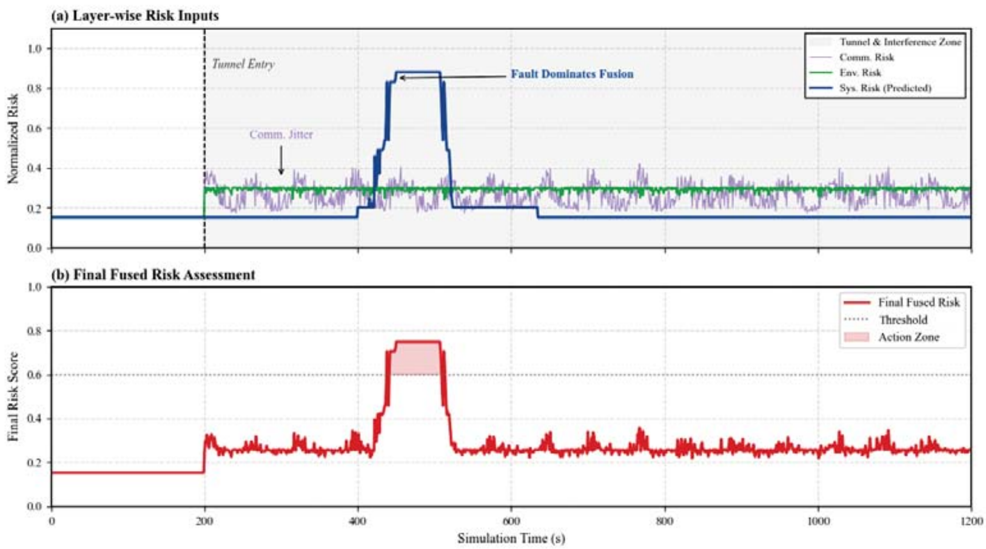

Fig. 4. **Multi-source Risk Fusion Results.**

preventing critical hazards from being masked by minor disturbances.

Preemptive Control Response. Fig. 5 presents the speed trajectories of the leading and following trains together with the corresponding MPC control actions. As shown in the left panel of Fig. 5, the following train exhibits an anticipatory deceleration and maintains a lower speed than the leading train during the high-risk interval (420 s $< t < 520$ s), thereby enlarging the safety margin. The right panel illustrates the associated control inputs, where moderate braking is applied in advance and followed by small corrective accelerations. During the recovery phase ($t > 550$ s),

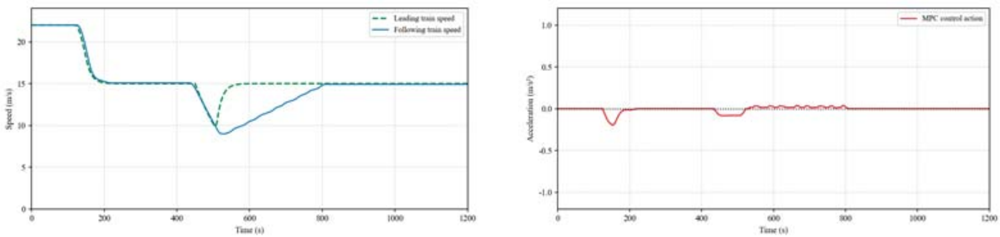

Fig. 5. **Speed control response under failure.** Left: speed trajectories of leading and following trains. Right: MPC control actions.

the following train returns to the nominal speed smoothly without aggressive catch-up, which supports robust longitudinal stability under degraded operating conditions.

5. Conclusions

This paper proposes a heterogeneous risk-aware fusion and control framework for virtual coupling operations under multi-source operational risks. By integrating multi-layer risk assessment, conservative Bi-CUSUM-based prediction, and MPC-based control framework, the framework enables preemptive and fail-safe longitudinal control for the following train. Simulation results demonstrate that the proposed approach provides safe and robust control performance in virtual coupling scenarios.

Acknowledgement

This work was supported by National Natural Science Foundation of China Regional Innovation Joint Fund Key Project (U22A2053), Guangxi Key R&D Project (Gui scientificAB 23075209) and the State Key Laboratory of Advanced Rail Autonomous Operation (Project No.RAO2026K03).

References

de Loizaga, G. C. R. and E. R. Martin (2024). State of the art of the future railway mobile communication system (frmcs) based on 5g technology. *Int. J. Sci. Acad. Res 5*, 7833–7840.

Farooq, J. and J. Soler (2017). Radio communication for communications-based train control (cbtc): A tutorial and survey. *IEEE Communications Surveys & Tutorials 19*(3), 1377–1402.

Felez, J., M. A. Vaquero-Serrano, and J. de Dios Sanz (2022). A robust model predictive control for virtual coupling in train sets. *Actuators 11*(12), 372.

Germoglio Barbosa, I., A. d. O. Lima, J. R. Edwards, and M. S. Dersch (2024). Development of track component health indices using image-based railway track inspection data. *Proceedings of the Institution of Mechanical Engineers, Part F: Journal of Rail and Rapid Transit 238*(6), 706–716.

Kong, R., S. Sahoo, F. Blaabjerg, X. Lyu, and X. Wang (2023). Controller stability and low-frequency interaction analysis of railway train-network systems. In *2023 25th European Conference on Power Electronics and Applications (EPE'23 ECCE Europe)*, pp. 1–9. IEEE.

Ning, B., H. Dong, S. Gao, et al. (2018). Distributed cooperative control of multiple high-speed trains under a moving block system by nonlinear mapping-based feedback. *Science China Information Sciences 61*(12), 120202.

Palo, M. (2014). *Condition-based maintenance for effective and efficient rolling stock capacity assurance: a study on heavy haul transport in Sweden*. Ph. D. thesis, Luleå tekniska universitet.

Su, S., W. Liu, Q. Zhu, et al. (2022). A cooperative collision-avoidance control methodology for virtual coupling trains. *Accident Analysis & Prevention 173*, 106703.

Su, S., J. She, K. Li, X. Wang, and Y. Zhou (2022). A nonlinear safety equilibrium spacing-based model predictive control for virtually coupled train set over gradient terrains. *IEEE Transactions on Transportation Electrification 8*(2), 2810–2824.

Xun, J., Y. Li, R. Liu, Y. Li, and Y. Liu (2022). A survey on control methods for virtual coupling in railway operation. *IEEE Open Journal of Intelligent Transportation Systems 3*, 838–855.

Zhu, L., D. Huang, X. Li, and Q. Wang (2024). Cooperative operation control of virtual coupling high-speed trains with input saturation and full-state constraints. *IEEE Transactions on Automation Science and Engineering 21*(3), 3497–3510.